Inorganic Chemistry

ARTICLE

pubs.acs.org/IC

Synthesis, Structure, and Spectroscopic Characterization of $[H_{8-n}Rh_{22}(CO)_{35}]^{n-}$ (n = 4, 5) and $[H_2Rh_{13}(CO)_{24}\{Cu(MeCN)\}_2]^-$ Clusters: Assessment of CV and DPV As Techniques to Circumstantiate the Presence of Elusive Hydride Atoms

Davide Collini,[†] Fabrizia Fabrizi De Biani,[‡] Dmitriy S. Dolzhnikov,[†] Cristina Femoni,*[,†] Maria C. Iapalucci,[†] Giuliano Longoni,[†] Cristina Tiozzo,[†] Stefano Zacchini,[†] and Piero Zanello[‡]

[†]Dipartimento di Chimica Fisica ed Inorganica, Università di Bologna, viale Risorgimento 4, 40136 Bologna, Italy

[‡]Dipartimento di Chimica, Università di Siena, via A. Moro, 53100 Siena, Italy

Supporting Information

ABSTRACT: The previously ill-characterized $[H_xRh_{22}(CO)_{35}]^{4-/5-}$ carbonyl cluster has been obtained as a byproduct of the synthesis of $[H_3Rh_{13}(CO)_{24}]^{2-}$ and effectively separated by metathesis of their sodium salts with $[NEt_4]Cl$. Although the yields are modest and never exceed 10−15% (based on Rh), this procedure affords spectroscopically pure $[H_3Rh_{22}(CO)_{35}]^{5-}$ anion. Formation of the latter in mixture with other Rh clusters was also observed by electrospray ionization-mass spectrometry (ESI-MS) in the oxidation of $[H_2Rh_{13}(CO)_{24}]^{3-}$ with Cu^{2+} salts. The recovery of further amounts of $[H_3Rh_{22}(CO)_{35}]^{5-}$ was hampered by too similar solubility of the salts composing the mixture. Conversely, the reaction in CH_3CN of $[H_2Rh_{13}(CO)_{24}]^{3-}$ with $[Cu(MeCN)_4]^+[BF_4]^-$ leads to the $[H_2Rh_{13}(CO)_{24}\{Cu(MeCN)\}_2]^-$ bimetallic cluster. The X-ray crystal structures of $[H_4Rh_{22}(CO)_{35}]^{4-}$, $[H_3Rh_{22}(CO)_{35}]^{5-}$, and $[H_2Rh_{13}(CO)_{24}\{Cu(MeCN)\}_2]^-$ are reported. From a formal point of view, the metal frame of the former two species can be derived by interpenetration along two orthogonal axes of two moieties displaying the structure of the latter. The availability of $[H_{8-n}Rh_{22}(CO)_{35}]^{n-}$ salts prompted their detailed chemical, spectroscopic, and electrochemical characterization. The presence of hydride atoms has been directly proved both by ESI-MS and ^1H NMR. Moreover, both $[H_4Rh_{22}(CO)_{35}]^{4-}$ and $[H_3Rh_{22}(CO)_{35}]^{5-}$ undergo distinctive electrochemically reversible redox changes. This allows to assess electrochemical studies as indisputable though circumstantial evidence of the presence of ^1H NMR-silent hydride atoms in isostructural anions of different charge.

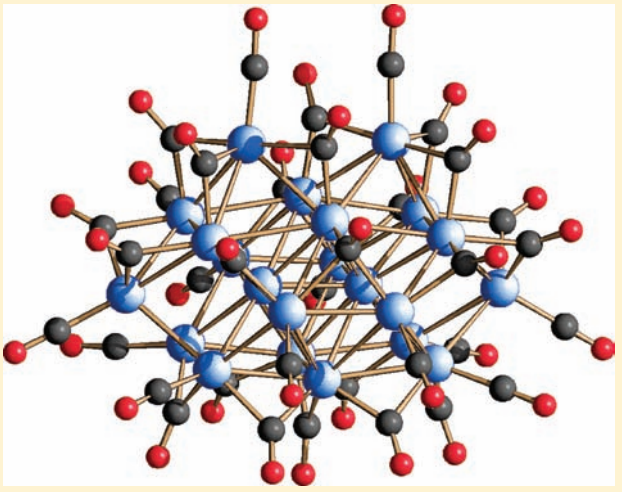

INTRODUCTION

Several rhodium carbonyl clusters containing interstitial Rh atoms are known, viz. $[H_3Rh_{13}(CO)_{24}]^{2-}$,[1,2] $[H_{4-n}Rh_{14}(CO)_{25}]^{n-}$ (n = 3, 4),[3,4] $[Rh_{14}(CO)_{26}]^{2-}$,[5,6] $[Rh_{15}(CO)_{27}]^{3-}$ (two isomers),[3,7] $[Rh_{15}(CO)_{25}(MeCN)_2]^{3-}$,[7] $[Rh_{15}(CO)_{30}]^{3-}$,[8] $[Rh_{17}(CO)_{30}]^{3-}$,[9] $[H_xRh_{22}(CO)_{35}]^{4-/5-}$,[10] and $[Rh_{22}(CO)_{37}]^{4-}$.[11] All above species contain a single interstitial Rh atom with the notable exception of the ill-characterized $[H_xRh_{22}(CO)_{35}]^{4-/5-}$ cluster, which comprise two interstitial Rh atoms. Our interest in the redox behavior of metal carbonyl clusters, and the finding that this is enhanced by the presence of interstitial metal atoms, prompted a reinvestigation of the ill-defined $[H_xRh_{22}(CO)_{35}]^{4-/5-}$ compound.

As a result, we report a new selective synthesis of $[H_xRh_{22}(CO)_{35}]^{4-/5-}$ species and their complete spectroscopic characterization as members of the $[H_{8-n}Rh_{22}(CO)_{35}]^{n-}$ (n = 3−7) series of clusters, undergoing acid−base equilibria in solution as a function of basicity of the solvent. Besides, each species of the above series undergoes several electrochemically reversible redox changes. The structure of the structurally related $[H_2Rh_{13}(CO)_{24}\{Cu(MeCN)\}_2]^-$ derivative is also reported.

RESULTS AND DISCUSSION

1. Synthesis of $[H_{8-n}Rh_{22}(CO)_{35}]^{n-}$ (n = 3−7) and $[H_2Rh_{13}(CO)_{24}\{Cu(MeCN)\}_2]^-$. A modification of the isolation procedure of $[H_3Rh_{13}(CO)_{24}]^{2-}$ allows one to obtain the concomitant isolation of $[H_3Rh_{22}(CO)_{35}]^{5-}$. The original syntheses of $[H_3Rh_{13}(CO)_{24}]^{2-}$ were based on mild pyrolysis of $Na_2[Rh_{12}(CO)_{30}]$ or reduction of $Rh_4(CO)_{12}$ with NaOH in isopropyl alcohol under a hydrogen atmosphere, followed by fractional precipitation of the resulting alkali salts from aqueous solution.[1,12] We confirmed that the above reactions mainly afford

Received: September 12, 2010
Published: February 11, 2011

$[H_3Rh_{13}(CO)_{24}]^{2-}$ (ca. 80−85% of starting Rh). However, a change in the isolation procedure allowed one to show that the most missing Rh is present as $[H_3Rh_{22}(CO)_{35}]^{5-}$. The change consists in the precipitation of the reaction mixture resulting from above reactions with tetraethyl ammonium chloride without any preventive fractional separation of their alkali salts. Owing to differential solubility of their tetraethylammonium salts, the $[NEt_4]_2[H_3Rh_{13}(CO)_{24}]$ salt is quantitatively extracted by THF, whereas the $[NEt_4]_5[H_3Rh_{22}(CO)_{35}]$ residue is only soluble in acetone and can be crystallized by layering isopropyl alcohol. The yields are only moderate (ca. 10−15% calcd on Rh) but the effective separation makes $[H_3Rh_{22}(CO)_{35}]^{5-}$ reproducibly available in workable amounts.

The corresponding $[H_4Rh_{22}(CO)_{35}]^{4-}$ salt has been obtained by protonation of $[H_3Rh_{22}(CO)_{35}]^{5-}$ in acetone with diluted H_3PO_4 and has been crystallized by layering isopropyl alcohol. Other salts with miscellaneous tetrasubstituted ammonium cations have been obtained by metathesis via addition of an aqueous solution of their halides to an acetone solution of $[NEt_4]_4[H_4Rh_{22}(CO)_{35}]$. Solutions of the tetrasubstituted ammonium salts of $[H_4Rh_{22}(CO)_{35}]^{4-}$ show infrared terminal carbonyl absorptions at 1992(s) and 1848(ms) cm^{-1}, whereas the parent $[H_3Rh_{22}(CO)_{35}]^{5-}$ salts exhibit absorptions at 1975(s) and 1837(ms) cm^{-1} with marginal variations as a function of the solvent.

As it will be discussed in Section 4, their structures are practically identical to that of the ill-characterized $[H_xRh_{22}(CO)_{35}]^{4-/5-}$ cluster, which was originally obtained by carbonylation at atmospheric CO pressure and high temperature (155 °C) of $Rh(CO)_2(acac)$ in the presence of cesium benzoate on using 18-crown-6 as solvent. This was isolated as $[Cs(18\text{-crown-}6)]^+$ salt and characterized as a $[H_xRh_{22}(CO)_{35}]^{4-/5-}$ cocrystallized 1:1 mixture.[10]

In the attempt to improve the yields of $[H_{8-n}Rh_{22}(CO)_{35}]^{n-}$, we investigated the oxidation of $[H_{5-n}Rh_{13}(CO)_{24}]^{n-}$ ($n = 2, 3$) with Fe^{3+} and Cu^{2+} salts. The results have not been rewarding owing to formation of inseparable mixtures of clusters, comprising also some Rh_{22} species. Only the attempted oxidation of $[H_2Rh_{13}(CO)_{24}]^{3-}$ with $[Cu(MeCN)_4]BF_4$ in acetonitrile or THF solution selectively affords the new $[H_2Rh_{13}(CO)_{24}\{Cu(MeCN)\}_2]^-$ cluster, according to eq 1

$$[H_2Rh_{13}(CO)_{24}]^{3-} + 2[Cu(MeCN)_4]^+ \rightarrow [H_2Rh_{13}(CO)_{24}\{Cu(MeCN)\}_2]^- + 6MeCN \quad (1)$$

The $[H_2Rh_{13}(CO)_{24}\{Cu(MeCN)\}_2]^-$ bimetallic cluster has been isolated in high yields by evaporation of the reaction solvent and crystallization of the residue from acetone/isopropyl alcohol mixtures.

The $[NEt_4][H_2Rh_{13}(CO)_{24}\{Cu(MeCN)\}_2]$ salt shows slightly different IR carbonyl absorptions in the miscellaneous organic solvents such as THF (ν_{CO} at 2013s, 2005s, 1921m, 1885m, 1869m, and 1853mw cm^{-1}), acetone (ν_{CO} at 2022sh, 2010s, 1923m, 1869m, 1853m and 1842m cm^{-1}), and acetonitrile (ν_{CO} at 2008s, 1980sh, 1897 m, 1838 m and 1824 m cm^{-1}) probably owing to solvent-exchange effects.

2. Chemical Properties of $[H_4Rh_{22}(CO)_{35}]^{4-}$. The $[H_{8-n}Rh_{22}(CO)_{35}]^{n-}$ ($n = 4, 5$) clusters are members of a wider series of compounds for which n assumes all values in the 2−7 range. These species have been obtained from $[H_4Rh_{22}(CO)_{35}]^{4-}$ according to eqs 2 and 3. Indeed, $[H_4Rh_{22}(CO)_{35}]^{4-}$ undergoes two completely reversible deprotonation processes. These are clearly signaled by stepwise lowering of ca. 15 cm^{-1} of the infrared carbonyl absorptions in each step (eq 2). The first deprotonation step gives $[H_3Rh_{22}(CO)_{35}]^{5-}$ and it partially or completely occurs on dissolving $[H_4Rh_{22}(CO)_{35}]^{4-}$ salts in acetonitrile, DMF, or DMSO, respectively. The subsequent deprotonation of $[H_3Rh_{22}(CO)_{35}]^{5-}$ requires stoichiometric addition of bases such as OH^- or OR^-. Of the resulting $[H_2Rh_{22}(CO)_{35}]^{6-}$ and $[HRh_{22}(CO)_{35}]^{7-}$ species, only the former could be isolated in a pure state, because the latter reconverts in its parent compound in the presence of water.

$$[H_4Rh_{22}(CO)_{35}]^{4-} \underset{H^+}{\overset{DMSO}{\rightleftharpoons}} [H_3Rh_{22}(CO)_{35}]^{5-} \underset{H^+}{\overset{OH^-}{\rightleftharpoons}} [H_2Rh_{22}(CO)_{35}]^{6-} \underset{H_2O}{\overset{OH^-}{\rightleftharpoons}} [HRh_{22}(CO)_{35}]^{7-} \quad (2)$$

$\nu CO\ (cm^{-1})$ 1992s, 1848ms 1975s, 1837ms 1958s, 1810ms 1945s, 1792ms

On the other side, there are analogous circumstantial evidence that $[H_4Rh_{22}(CO)_{35}]^{4-}$ undergoes at least two reversible protonation processes, as suggested by two stepwise increase of ca. 15 cm^{-1} of the infrared carbonyl absorptions upon addition of acids in acetone (eq 3).

$$[H_4Rh_{22}(CO)_{35}]^{4-} \underset{MeCN}{\overset{H^+}{\rightleftharpoons}} [H_5Rh_{22}(CO)_{35}]^{3-} \underset{Me_2CO}{\overset{H^+}{\rightleftharpoons}} [H_6Rh_{22}(CO)_{35}]^{2-} \quad (3)$$

$\nu CO\ (cm^{-1})$ 1992s, 1848ms 2008s, 1864ms 2022s, 1895ms

Of these, only $[H_5Rh_{22}(CO)_{35}]^{3-}$ could be isolated in a spectroscopically pure state, whereas $[H_6Rh_{22}(CO)_{35}]^{2-}$ was always obtained in mixture with the parent compound owing to its ready deprotonation in most organic solvents.

As it will be shown in Section 5, the $[H_{8-n}Rh_{22}(CO)_{35}]^{n-}$ ($n = 4, 5$) clusters also undergo reversible redox changes. A further reason of interest in their chemical reactivity stems from their complex transformations under an atmosphere of either H_2 or CO, as well as their reaction with unsaturated substrates such as phenylacetylene and styrene. Unravelling of all above transformations will require much future work.

3. ^{1}H NMR Characterization of $[H_{8-n}Rh_{22}(CO)_{35}]^{n-}$ ($n = 4, 5$) and $[H_2Rh_{13}(CO)_{24}\{Cu(MeCN)\}_2]^-$. Direct observation of the purported hydride atoms by ^{1}H NMR of $[H_{8-n}Rh_{22}(CO)_{35}]^{n-}$ ($n = 4, 5$) has been rather troublesome, probably because their nuclearity is close to the upper limit (ca. 20−25 metal atoms) at which multinuclear NMR experiments of most metal carbonyl anionic clusters result silent.[13] The observation of their hydride signals is only possible by using a 600 MHz instrument with the most sensitive probe and thousands of pulses. The ^{1}H NMR in d^3-acetonitrile of $[H_3Rh_{22}(CO)_{35}]^{5-}$ in its NEt_4^+ salt displays a broad hydride signal at δ −23.5 ppm. The corresponding $[NEt_4]_4[H_4Rh_{22}(CO)_{35}]$ salt in d^6-acetone shows a related signal at δ −14.4 ppm. Both signals are rather broad (half-widths in the 100−250 Hz range) and the expected coupling with ^{103}Rh could not be resolved. No ^{1}H NMR signal corresponding to the one reported in a note (τ 29.5, δ −19.5) for $[H_xRh_{22}(CO)_{35}]^{4-/5-}$ was observed.[10] The possible occurrence in solution of intermolecular proton-exchange was ruled out by recording the ^{1}H NMR of a d^3-acetonitrile solution of $[NEt_4]_4[H_4Rh_{22}(CO)_{35}]$, which partially dissociates in $[H_3Rh_{22}(CO)_{35}]^{5-}$ in such solvent. The ^{1}H NMR spectrum (see Figure 1a) at room temperature shows two distinct ^{1}H NMR signals corresponding to those of $[H_3Rh_{22}(CO)_{35}]^{5-}$ and $[H_4Rh_{22}(CO)_{35}]^{4-}$. Conversely, as shown in Figure 1b, the ^{1}H NMR of the above sample in d^6-DMSO is consistent with IR observations (see eq 2) by showing the complete dissociation of $[H_4Rh_{22}(CO)_{35}]^{4-}$ into its $[H_3Rh_{22}(CO)_{35}]^{5-}$ conjugate base.

The suggested number of hydride atoms of each species could not be established by integration, and the proposed $[H_{8-n}Rh_{22}(CO)_{35}]^{n-}$ general formula is based on other direct and indirect

dx.doi.org/10.1021/ic101872z |Inorg. Chem. 2011, 50, 2790–2798

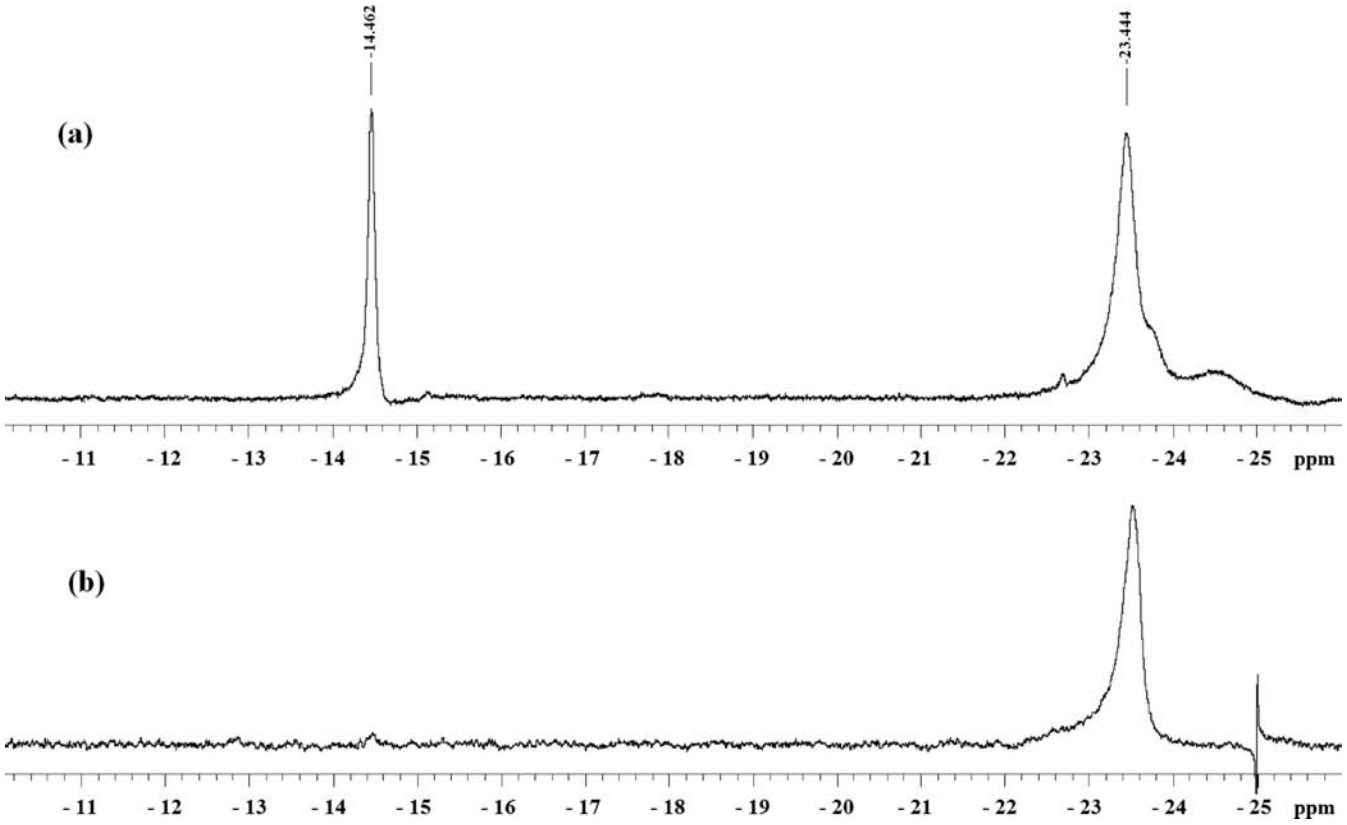

Figure 1. The ^{1}H NMR spectra of $[H_4Rh_{22}(CO)_{35}]^{4-}$, signal at δ −14.462 ppm, which partially dissociates to its parent $[H_3Rh_{22}(CO)_{35}]^{5-}$ pentaanion in d^3-acetonitrile solution, signal at δ −23.444 ppm (a); the dissociation is complete in d^6-DMSO solution (b).

evidence (vide infra). For instance, the presence of at least three hydride atoms in $[H_4Rh_{22}(CO)_{35}]^{4-}$ is circumstantiated by the number of reversible deprotonation equilibria described in eq 3.

A second direct proof of the presence of hydride atoms in $[H_{8-n}Rh_{22}(CO)_{35}]^{n-}$ (n = 4, 5), as well as $[H_2Rh_{13}(CO)_{24}\{Cu(MeCN)\}_2]^-$, is provided by electrospray ionization-mass spectrometry (ESI-MS) experiments, as detailed in the Supporting Information.

The $[NEt_4][H_2Rh_{13}(CO)_{24}\{Cu(MeCN)\}_2]$ adduct exhibits a single signal at δ −26.6 ppm in d^6-acetone at RT, which shifts at −27.3 ppm by lowering the temperature at −40 °C. In contrast, in d^3-acetonitrile solution shows a signal at −29.03 ppm from RT to −20 °C. These signals are also rather broad and do not show hyperfine structures.

The fact that a single signal is systematically observed for the above $[H_{8-n}Rh_{22}(CO)_{35}]^{n-}$ (n = 4, 5) and $[H_2Rh_{13}(CO)_{24}\{Cu(MeCN)\}_2]^-$ polyhydride derivatives probably arises from fast site-exchange of all hydride atoms in the investigated range of temperatures as for the parent $[H_{5-n}Rh_{13}(CO)_{24}]^{n-}$ (n = 2, 3) clusters.[12]

4. X-ray Structures of $[H_4Rh_{22}(CO)_{35}]^{4-}$, $[H_3Rh_{22}(CO)_{35}]^{5-}$, and $[H_2Rh_{13}(CO)_{24}\{Cu(MeCN)\}_2]^-$. The description of the structure of $[H_2Rh_{13}(CO)_{24}\{Cu(MeCN)\}_2]^-$ is anticipated owing to its structural relationship with $[H_{8-n}Rh_{22}(CO)_{35}]^{n-}$ (n = 4,5).

4.1. Structure of $[NEt_4][H_2Rh_{13}(CO)_{24}\{Cu(MeCN)\}_2]$. The structure of the $[H_2Rh_{13}(CO)_{24}\{Cu(MeCN)\}_2]^-$ monoanion with numbering scheme is given in Figure 2 and the M−M interatomic distances are collected in Table 1, whereas the full list of bonds is given in the Supporting Information as Table S1.

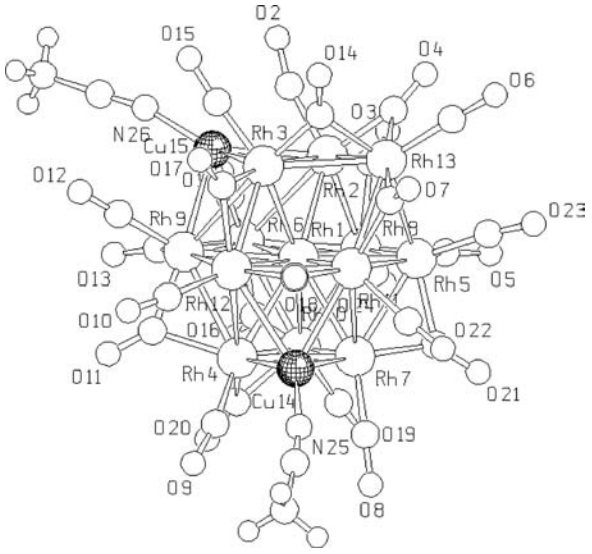

Figure 2. The crystal structure of $[H_2Rh_{13}(CO)_{24}\{Cu(MeCN)\}_2]^-$ anion with numbering scheme (carbon atoms are numbered as their corresponding oxygen atoms).

As illustrated in Figure 3, where also Rh−Rh contacts in the 3.00−3.25 Å are included, the resulting metal frame may be envisioned as deriving from the fusion of a bicapped body-centered cubic (top half) and a close-packed (bottom half) moiety. The description points out the presence in the Cu_2Rh_{13} metal frame of two octahedral cavities of Rh_6 and $CuRh_5$ composition

dx.doi.org/10.1021/ic101872z |*Inorg. Chem.* 2011, 50, 2790–2798

Table 1. Bond Distances (Å) within the $[H_2Rh_{13}(CO)_{24}\{Cu(MeCN)\}_2]^-$ Anion

Rh(1)−Rh(7)	2.635(2)
Rh(1)−Rh(9)	2.636(2)
Rh(1)−Rh(2)	2.651(2)
Rh(1)−Rh(6)	2.656(2)
Rh(1)−Rh(3)	2.669(2)
Rh(1)−Rh(10)	2.689(2)
Rh(1)−Rh(11)	2.690(2)
Rh(1)−Rh(5)	2.691(2)
Rh(1)−Rh(4)	2.725(2)
Rh(1)−Rh(8)	2.901(3)
Rh(1)−Rh(12)	2.975(3)
Rh(2)−Rh(8)	2.729(2)
Rh(2)−Rh(13)	2.803(2)
Rh(2)−Rh(3)	2.826(3)
Rh(2)−Rh(6)	3.044(3)
Rh(3)−Rh(12)	2.730(2)
Rh(3)−Rh(13)	2.811(3)
Rh(3)−Rh(9)	2.998(3)
Rh(4)−Rh(7)	2.688(2)
Rh(4)−Rh(10)	2.757(3)
Rh(4)−Rh(9)	2.758(2)
Rh(4)−Rh(12)	2.817(3)
Rh(5)−Rh(7)	2.708(2)
Rh(5)−Rh(8)	2.742(2)
Rh(5)−Rh(13)	2.819(3)
Rh(5)−Rh(11)	2.904(3)
Rh(6)−Rh(8)	2.691(2)
Rh(6)−Rh(9)	2.770(3)
Rh(6)−Rh(10)	2.781(2)
Rh(7)−Rh(10)	2.639(2)
Rh(7)−Rh(11)	2.737(3)
Rh(8)−Rh(10)	2.750(2)
Rh(9)−Rh(12)	2.721(2)
Rh(11)−Rh(12)	2.742(3)
Rh(11)−Rh(13)	2.773(3)
Rh(2)−Cu(15)	2.638(3)
Rh(3)−Cu(15)	2.648(3)
Rh(4)−Cu(14)	2.593(3)
Rh(6)−Cu(15)	2.630(3)
Rh(7)−Cu(14)	2.648(3)
Rh(9)−Cu(15)	2.651(3)
Rh(11)−Cu(14)	2.653(3)
Rh(12)−Cu(14)	2.707(3)

in the top half in addition to the octahedral $CuRh_5$ cavity of the bottom half.

The ligand stereochemistry comprises 12 terminal and 12 bridging COs as in the starting $[H_2Rh_{13}(CO)_{24}]^{3-}$ cluster, as well as 2 terminal acetonitrile ligands bonded to the 2 Cu atoms. In particular, the two square faces adjacent to those capped by $[Cu(MeCN)]^+$ display all four edges spanned by bridging carbonyls. The remaining two share one bridging CO and additionally display one or two edges spanned by bridging carbonyls, respectively. It is worth noting that CO(3) and CO(15) lean toward Cu(15) and show Cu−C contacts of 2.27 and 2.34 Å, respectively (these loose contacts have been arbitrarily omitted

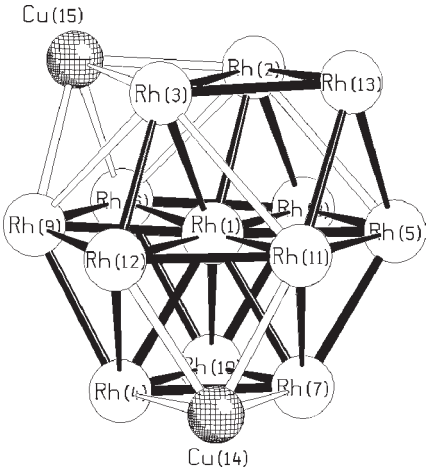

Figure 3. A view of the Cu_2Rh_{13} metal framework pointing out the bicapped body-centered cubic distortion of the upper half (Rh−Rh bonds shown as open bond sticks represent loose contacts comprised in the 3.00−3.25 Å range).

in Figure 3). The drawing of these short contacts reinforces the formal derivation of the structure of $[H_4Rh_{22}(CO)_{35}]^{4-}$ from interpenetration of two Rh_{15} moieties displaying the structure of $[H_2Rh_{13}(CO)_{24}\{Cu(MeCN)\}_2]^-$.

As a result, The M_{15} framework of $[H_2Rh_{13}(CO)_{24}\{Cu(MeCN)\}_2]^-$ is roughly similar but yet different from those displayed by known isonuclear and nonisoelectronic homo- and bimetallic Rh clusters, for example, $[Rh_{15}(CO)_{27}]^{3-}$ (two isomers; 192 CVE),[3,7] $[Rh_{15}(CO)_{25}(MeCN)_2]^{3-}$ (192 CVE),[7] $[NiRh_{14}(CO)_{28}]^{4-}$ (196 CVE)[14] and $[Rh_{15}(CO)_{30}]^{3-}$ (198 CVE).[8] Actually, it completes the above series by providing an example of cluster with 194 cluster valence electrons (CVE) and shows that even relatively small distortions of the metal frame may affect the electron count of isonuclear metal carbonyl clusters and vice versa.

A neutron diffraction analysis of the parent $[H_2Rh_{13}(CO)_{24}]^{3-}$[15,16] confirmed the suggestion made by X-ray diffraction that the hydride atoms were lodged in the most expanded square pyramidal moieties.[2] In the case of $[H_2Rh_{13}(CO)_{24}\{Cu(MeCN)\}_2]^-$, owing to the above distortions, the number of square pyramidal cavities is reduced to two and they are both in the bottom half of the cluster. Moreover, there are one Rh_6 and two nonequivalent $CuRh_5$ octahedral cavities. As a result, there are no equivalent cavities present in the cluster. The fact that two hydride atoms are equivalent in solution (see Section 3) may be therefore due to either fortuitous magnetic equivalence or rapid motion between the above cavities.

4.2. Structure of $[NMe_3CH_2Ph]_4[H_4Rh_{22}(CO)_{35}]$. The unit cell of $[NMe_3CH_2Ph]_4[H_4Rh_{22}(CO)_{35}]$ consists of an ionic packing of two cluster anions and eight $[NMe_3CH_2Ph]^+$ cations with normal van der Waals contacts. The structure of the tetraanion and the numbering scheme is given in Figure 4 and Rh−Rh distances are collected in Table 2, whereas the full list of bonds is provided as Table S2 in the Supporting Information.

The metal framework may be described as a distorted chunk of a body-centered cubic lattice and formally derives from the fusion of two rhodium-centered cubes, which generates a tetragonal prism capped on all but two adjacent square faces by Rh atoms. The overall structure is almost coincident with that reported for the cocrystallized $[H_xRh_{22}(CO)_{35}]^{4-/5-}$ mixture.[10] Only minor

dx.doi.org/10.1021/ic101872z |*Inorg. Chem.* 2011, 50, 2790–2798

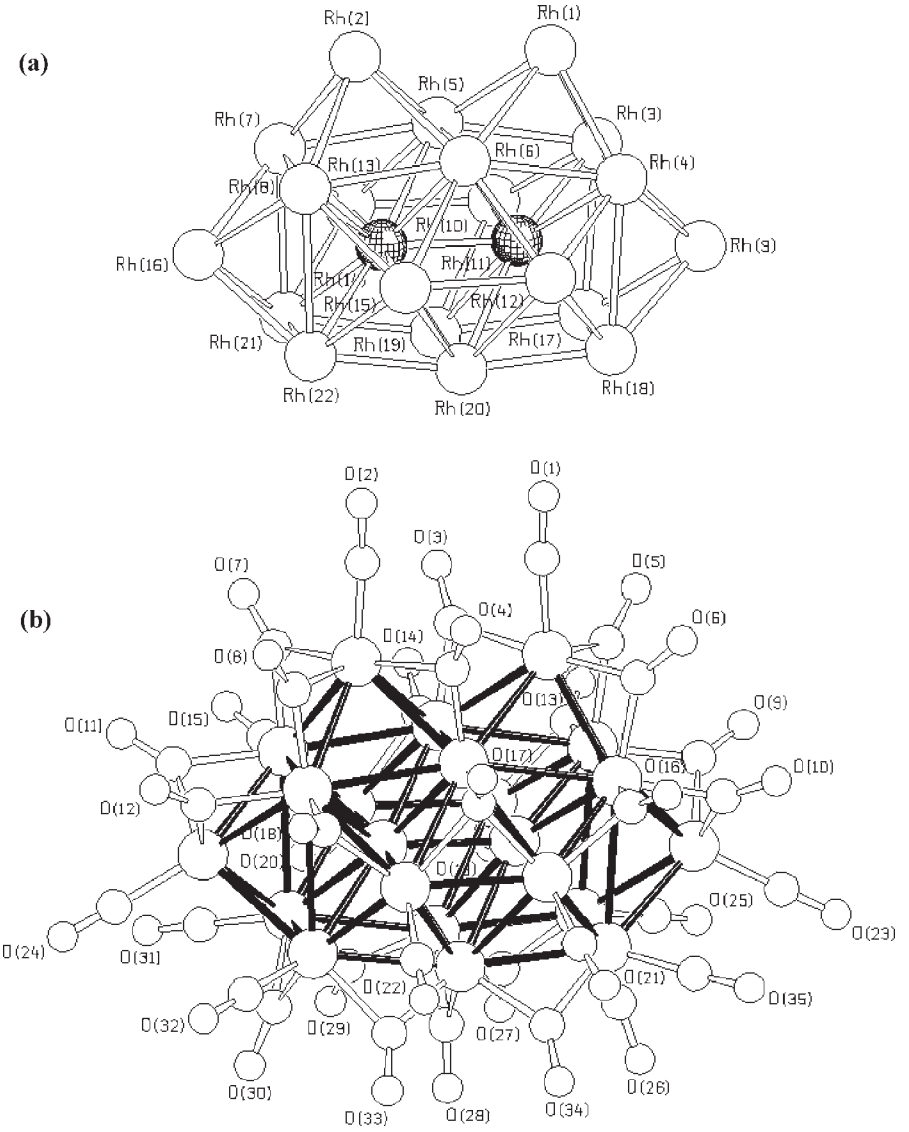

Figure 4. Metal framework (a) and structure (b) of the $[H_4Rh_{22}(CO)_{35}]^{4-}$ anion with numbering scheme (carbon atoms are numbered as their corresponding oxygen atoms).

differences can be noticed. Thus, the overall idealized symmetry of the $[H_4Rh_{22}(CO)_{35}]^{4-}$ tetraanion is only C_2 with the 2-fold axis passing through the midpoints of the Rh(5)−Rh(6) and Rh(19)−Rh(20) edges, rather than C_{2v} as for the cocrystallized $[H_xRh_{22}(CO)_{35}]^{4-/5-}$ mixture. The reduced idealized symmetry is due to unsymmetrical Rh−Rh contacts of the Rh(1) and Rh(2) caps (see Table 2 and Supporting Information S2). Their unique Rh−Rh edge not spanned by a μ-CO ligand (2.87 Å, on average) is longer than the average of the other three spanned by μ-CO (2.76 Å). Furthermore, CO(3) and CO(4) are unsymmetrical edge-bridges (average Rh−C 1.90 and 2.23 Å) leaning toward a third metal atom (Rh···C 2.74 Å), rather than terminally bonded to the hinge rhodium atom and leaning toward the two rhodium caps. These small distortions cause the loss of a crystallographic mirror plane.

The Rh−Rh distances are rather scattered and range from 2.480(2) to 3.14 Å. The shortest contact is the one connecting the two interstitial Rh(11) and Rh(14) atoms, while the longest distance represents the average of the four vertical edges of the tetragonal prism.

The Rh(1)−Rh(2) contact (3.601 Å) is clearly nonbonding. The $[H_{8-n}Rh_{22}(CO)_{35}]^{n-}$ (n = 4, 5) cluster with its 276 CVE is isoelectronic but not isostructural with $[Rh_{22}(CO)_{37}]^{4-}$,[11] which features only one interstitial Rh atom. Conversely, it is isoelectronic as well as isostructural with $[Rh_{18}Pt_4(CO)_{35}]^{4-}$,[17] in which the four Pt atoms describe a tetrahedron and are located in the interstitial sites and at the hinge in correspondence of the Rh(5), Rh(6), Rh(11), and Rh(14) atoms of Figure 4b. The unusually short M−M contact between the respective interstitial atoms of $[H_4Rh_{22}(CO)_{35}]^{4-}$ (Rh(11)−Rh(14) = 2.480(2) Å) and $[Rh_{18}Pt_4(CO)_{35}]^{4-}$ (Pt−Pt 2.559(1) Å) may appear puzzling. Rh−Rh interatomic separations in the range 2.39−2.61 Å in Rh(I) and Rh(II) dimers held together by bridging ligands (e.g., $HCOO^-$, CH_3COO^-, μ-PR_2, μ-CO) have previously been suggested to indicate the presence of Rh═Rh double bonds.[18−20] Such a proposal started a controversy. It seems now established on the basis of several theoretical calculations with miscellaneous methods[21] that the Rh−Rh bond is weak and sensitive to even small perturbations. As a result, it has been concluded that the above distances are shorter than expected simply because of the

dx.doi.org/10.1021/ic101872z |*Inorg. Chem.* 2011, 50, 2790–2798

Table 2. Bond Distances (Å) within the $[H_4Rh_{22}(CO)_{35}]^{4-}$ Anion

Rh(1)−Rh(3)	2.736(2)
Rh(1)−Rh(4)	2.750(2)
Rh(1)−Rh(5)	2.798(2)
Rh(1)−Rh(6)	2.876(2)
Rh(2)−Rh(8)	2.737(2)
Rh(2)−Rh(7)	2.745(2)
Rh(2)−Rh(6)	2.799(2)
Rh(2)−Rh(5)	2.869(2)
Rh(3)−Rh(11)	2.624(2)
Rh(3)−Rh(10)	2.636(2)
Rh(3)−Rh(9)	2.732(2)
Rh(3)−Rh(4)	2.833(2)
Rh(3)−Rh(5)	2.962(2)
Rh(3)−Rh(17)	3.148(2)
Rh(4)−Rh(11)	2.586(2)
Rh(4)−Rh(12)	2.647(2)
Rh(4)−Rh(9)	2.719(2)
Rh(4)−Rh(6)	2.916(2)
Rh(4)−Rh(18)	3.148(2)
Rh(5)−Rh(11)	2.674(2)
Rh(5)−Rh(14)	2.694(2)
Rh(5)−Rh(13)	2.759(2)
Rh(5)−Rh(10)	2.761(2)
Rh(5)−Rh(7)	2.908(2)
Rh(5)−Rh(6)	2.928(2)
Rh(6)−Rh(11)	2.669(2)
Rh(6)−Rh(14)	2.684(2)
Rh(6)−Rh(12)	2.735(2)
Rh(6)−Rh(15)	2.795(2)
Rh(6)−Rh(8)	2.950(2)
Rh(7)−Rh(14)	2.630(2)
Rh(7)−Rh(13)	2.670(2)
Rh(7)−Rh(16)	2.724(2)
Rh(7)−Rh(8)	2.873(2)
Rh(7)−Rh(21)	3.114(2)
Rh(8)−Rh(14)	2.634(2)
Rh(8)−Rh(15)	2.667(2)
Rh(8)−Rh(16)	2.701(2)
Rh(8)−Rh(22)	3.124(2)
Rh(9)−Rh(18)	2.784(2)
Rh(9)−Rh(17)	2.814(2)
Rh(10)−Rh(13)	2.648(2)
Rh(10)−Rh(17)	2.761(2)
Rh(10)−Rh(19)	2.898(2)
Rh(10)−Rh(11)	3.014(2)
Rh(11)−Rh(14)	2.480(2)
Rh(11)−Rh(17)	2.685(2)
Rh(11)−Rh(18)	2.685(2)
Rh(11)−Rh(19)	2.732(2)
Rh(11)−Rh(20)	2.736(2)
Rh(11)−Rh(12)	3.009(2)
Rh(12)−Rh(15)	2.646(2)
Rh(12)−Rh(18)	2.749(2)
Rh(12)−Rh(20)	2.922(2)
Rh(13)−Rh(21)	2.707(2)
Rh(13)−Rh(19)	2.894(2)
Rh(13)−Rh(14)	3.014(2)
Rh(14)−Rh(21)	2.614(2)
Rh(14)−Rh(22)	2.643(2)
Rh(14)−Rh(20)	2.734(2)
Rh(14)−Rh(19)	2.738(2)
Rh(14)−Rh(15)	2.966(2)
Rh(15)−Rh(22)	2.688(2)
Rh(15)−Rh(20)	2.832(2)
Rh(16)−Rh(21)	2.777(2)
Rh(16)−Rh(22)	2.800(2)
Rh(17)−Rh(19)	2.727(2)
Rh(17)−Rh(18)	2.815(2)
Rh(18)−Rh(20)	2.736(2)
Rh(19)−Rh(21)	2.778(2)
Rh(19)−Rh(20)	2.779(2)
Rh(20)−Rh(22)	2.787(2)
Rh(21)−Rh(22)	2.763(2)

presence of bridging ligands. This appears to be the case also for the above short Rh−Rh and Pt−Pt distances. Indeed, EHMO calculations on $[Rh_{22}(CO)_{35}]^{8-}$, by using the crystallographic coordinates of $[H_4Rh_{22}(CO)_{35}]^{4-}$, point out crowding of energy levels in the frontier region and a highest occupied molecular orbital−lowest unoccupied molecular orbital (HOMO−LUMO) gap of ca. 0.25 eV, which should grant a closed-shell electronic configuration. Analysis of the bond overlap populations indicates that the OP of Rh(11)−Rh(14) bond is only marginally superior to that of the other Rh−Rh bonds. Since each interstitial Rh is 11-coordinated and the short Rh(11)−Rh(14) interaction is spanned by 4 Rh atoms, emphasis on the meaning of such bond-length seems unjustified.

The $[H_4Rh_{22}(CO)_{35}]^{4-}$ has 276 CVE. Its metal frame may formally be obtained by interpenetrating two $[H_{4-n}Rh_{14}(CO)_{25}]^{n-}$ [3,4] (180 CVE) clusters and sharing of an octahedral Rh_6 moiety. This would imply Rh(1) and Rh(2) to be at bond distance, while they are 3.6 Å apart. According to Mingos condensation rules,[22] the expected electron count should be 180 × 2 − 86 = 274 CVE. It seems conceivable that the above bond is broken due to the presence of 2 extra CVE. More accurately, the structure of $[H_4Rh_{22}(CO)_{35}]^{4-}$ can be obtained by interpenetration along two almost orthogonal axes of two homonuclear Rh_{15} clusters, displaying the overall structure of $[H_2Rh_{13}(CO)_{24}\{Cu(MeCN)\}_2]^-$ (194 CVE). Such an interpenetration does not lead to formation of a Rh(1)····Rh(2) bond and would require sharing of a Rh_8 moiety, which comprises the Rh atoms labeled Rh(5), Rh(6), Rh(10), Rh(11), Rh(14), Rh(15), Rh(19), and Rh(20) of Figure 4b. This shared Rh_8 moiety essentially consisting of two square-pyramids sharing triangular faces with a tetrahedron is referable to the metal frame of $Ru_8S_2(CO)_{17}(C_6H_5Me)$,[23] which features 112 CVE. As a result, the predictable electron count of $[H_4Rh_{22}(CO)_{35}]^{4-}$ becomes 194 × 2 − 112 = 276 CVE, which is in agreement with the experimentally observed number.

4.3. Structure of $[NEt_4]_5[H_3Rh_{22}(CO)_{35}]\cdot 2Me_2CO$. The unit cell of $[NEt_4]_5[H_3Rh_{22}(CO)_{35}]\cdot 2Me_2CO$ consists of a ionic packing of 4 cluster anions $[H_3Rh_{22}(CO)_{35}]^{5-}$, 20 $[NEt_4]^+$

dx.doi.org/10.1021/ic101872z |*Inorg. Chem.* 2011, 50, 2790–2798

Table 3. Formal Redox Potentials (in V, vs SCE) of the Miscellaneous Reversible Redox Couples Featured by $[H_4Rh_{22}(CO)_{35}]^{4-}$ and $[H_3Rh_{22}(CO)_{35}]^{5-}$

compound	reductions				oxidations		solvent
$[H_3Rh_{22}(CO)_{35}]^{5-}$	−1.59	−1.41	−1.10	−0.65	−0.24	+0.18	DMF
$[H_3Rh_{22}(CO)_{35}]^{5-}$	−1.60	−1.38	−1.05	−0.60	−0.24		MeCN
$[H_4Rh_{22}(CO)_{35}]^{4-}$		−1.20	−0.82	−0.73	+0.01		MeCN

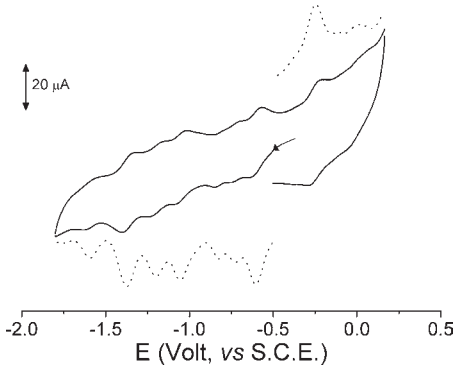

Figure 5. Cyclic (full line) and differential pulse voltammetry (dotted line) of a mixture of $[H_3Rh_{22}(CO)_{35}]^{5-}$ and $[H_4Rh_{22}(CO)_{35}]^{4-}$ in acetonitrile.

cations, and 8 acetone molecules with normal van der Waals contacts. The structure of the pentaanion is identical to that of the parent $[H_4Rh_{22}(CO)_{35}]^{4-}$ tetraanion and only marginally differs in some individual molecular parameter. Therefore, it is not discussed in any further detail. The numbering scheme and most relevant interatomic distances for $[NEt_4]_5[H_3Rh_{22}(CO)_{35}]\cdot 2Me_2CO$ are given in the Supporting Information as Figure S2 and Table S3.

5. Redox Properties of $[H_{8-n}Rh_{22}(CO)_{35}]^{n-}$ (n = 4, 5). Experimentally, $[H_2Rh_{13}(CO)_{24}\{Cu(MeCN)\}_2]^-$ only undergoes irreversible redox changes like the previously investigated $[H_3Rh_{13}(CO)_{24}]^{2-}$.[7] These seem to be also complicated by stripping processes of Cu. Conversely, both $[H_4Rh_{22}(CO)_{35}]^{4-}$ and $[H_3Rh_{22}(CO)_{35}]^{5-}$ exhibit a rich reversible redox chemistry, probably favored by the greater stability of their metal frames. The formal redox potentials of the miscellaneous reversible redox couples featured by $[H_4Rh_{22}(CO)_{35}]^{4-}$ and $[H_3Rh_{22}(CO)_{35}]^{5-}$ are collected in Table 3.

$[H_3Rh_{22}(CO)_{35}]^{5-}$ exhibits four reversible reductions and two reversible oxidations, whereas $[H_4Rh_{22}(CO)_{35}]^{4-}$ shows three reversible reductions and one reversible oxidation.

The cyclic voltammetry (CV) and differential pulse voltammetry (DPV) profiles of $[H_4Rh_{22}(CO)_{35}]^{4-}$ in acetonitrile and DMF are shown in Figures 5 and 6. In keeping with the occurrence in these solvents of the first equilibrium shown in eq 2, which is more or less shifted toward right as a function of the increasing basicity of the solvent, the profile of $[H_4Rh_{22}(CO)_{35}]^{4-}$ in acetonitrile exhibits up to nine reversible redox changes, which result from the presence in solution of residual $[H_4Rh_{22}(CO)_{35}]^{4-}$ (least intense set of peaks) and the corresponding $[H_3Rh_{22}(CO)_{35}]^{5-}$ conjugate base (most intense set of peaks). In Figure 6, the cathodic DPV profile of the above mixture is compared with that of the same sample in DMF. In this solvent, the first equilibrium of eq 2 is almost completely shifted toward right. Therefore, the DPV profile is that of $[H_3Rh_{22}(CO)_{35}]^{5-}$. The presence of some residual $[H_4Rh_{22}(CO)_{35}]^{4-}$ is here barely noticeable.

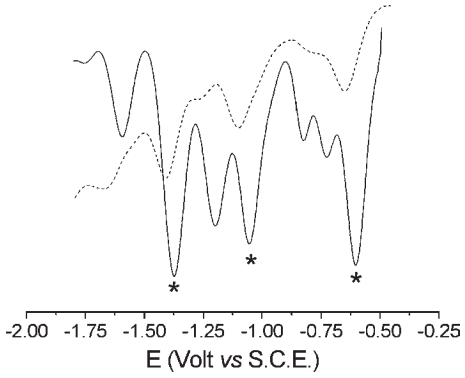

Figure 6. Comparison between the DPV profiles of $[H_4Rh_{22}(CO)_{35}]^{4-}$ in acetonitrile (full line) and DMF (dotted line).

Beyond other considerations, the experiments reported in Figures 5 and 6 and Table 3 demonstrate the complexity of the $[H_{8-n}Rh_{22}(CO)_{35}]^{n-}$ system which may comprise conjugate acids and bases and multiple oxidation states of each cluster species. Moreover, they show the valuable contribution that electrochemistry can give in unravelling the nature of isostructural anions differing in their charge. It can provide unambiguous, even if circumstantial, evidence of the presence of hydride atoms. Should, for instance, the isostructural tetra- and pentaanion be the respectively open- and closed-shell $[H_4Rh_{22}(CO)_{35}]^{5-}$ and $[H_4Rh_{22}(CO)_{35}]^{4-}$ pair of compounds, a steady-state profile only comprising one set of redox changes would have been observed. Observation in acetonitrile of two sets of distinct profiles, which reduce to one in a more basic solvent such as DMF, indisputably implements the occurrence in solution of the first equilibrium of eq 2 and demonstrates that the tetraanion is the conjugate acid of the pentaanion. The present results lend further support to previous conclusions drawn from related chemical and electrochemical behavior of other metal carbonyl clusters containing elusive hydride atoms[24−26] for which a direct proof (via ^{1}H NMR or ESI-MS) could not be obtained.

EXPERIMENTAL SECTION

All reactions including sample manipulations were carried out with standard Schlenk techniques under nitrogen and in carefully dried solvents. Analysis of Rh has been performed by atomic absorption on a Pye-Unicam instrument. Infrared spectra were recorded on a Perkin-Elmer 1605 interferometer using CaF_2 cells. EPR experiments were carried out on a Bruker ER 041 XG instrument. NMR spectra were recorded on Varian 400 and 600 MHz instruments and ESI-MS on a Waters ZQ-4000 instrument.

Cyclic voltammetry was performed in a three-electrode cell having a platinum working electrode surrounded by a platinum-spiral counter electrode and the aqueous saturated calomel reference electrode (SCE) mounted with a Luggin capillary. Either a BAS 100A or a BAS 100W electrochemical analyzer was used as a polarizing unit. Apparatus and materials for electrochemical measurements are described elsewhere.[27] Potential values are referred to the SCE. Under the present experimental conditions, the one-electron oxidation of ferrocene occurs at $E°$ = + 0.38 V in acetonitrile and +0.47 V in DMF.

EH calculations and structure drawings have been performed with CACAO98[28] and SCHAKAL99,[29] respectively.

1. Synthesis of $[H_3Rh_{22}(CO)_{35}]^{5-}$ from $Rh_4(CO)_{12}$. A solution of $Rh_4(CO)_{12}$ (1,99 g, 2.26 mmol) in diisopropyl alcohol (50 mL) and water (0.4 mL) was heated under H_2 after the addition of a solution of NaOH in diisopropyl alcohol (0.1 M, molar ratio OH^-/Rh = 2:13). The mixture was kept under reflux and vigorously stirred for 24 h. The

dx.doi.org/10.1021/ic101872z |Inorg. Chem. 2011, 50, 2790–2798

Table 4. Summary of Crystal Data for $[NMe_3CH_2Ph]_4[H_4Rh_{22}(CO)_{35}]$, $[NEt_4]_5[H_3Rh_{22}(CO)_{35}]\cdot 2Me_2CO$, and $[NEt_4][H_2Rh_{13}(CO)_{24}\{Cu(MeCN)\}_2]$

compound	$[NMe_3CH_2Ph]_4[H_4Rh_{22}(CO)_{35}]$	$[NEt_4]_5[H_3Rh_{22}(CO)_{35}]\cdot 2Me_2CO$	$[NEt_4][H_2Rh_{13}(CO)_{24}\{Cu(MeCN)\}_2]$
fw	3845.32	4009.76	2349.51
T, K	100(2)	100(2)	100(2)
λ, å	0.71073	0.71073	0.71073
crystal system	triclinic	monoclinic	triclinic
space group	$P\bar{1}$	$P2_1/n$	$P\bar{1}$
a, Å	14.627(3)	14.0031(9)	11.614(4)
b, Å	14.990(3)	29.5161(19)	12.114(5)
c, Å	23.881(4)	25.9818(16)	21.529(8)
α, °	79.105(4)	90	91.047(5)
β, °	78.150(4)	92.1930(10)	96.820(5)
γ, °	72.032(4)	90	117.562(4)
cell volume, Å^3	4829.9(15)	10730.9(12)	2657.1(17)
Z	2	4	2
D_c, g cm^{-3}	2.644	2.482	2.937
μ, mm^{-1}	3.723	3.358	4.780
F(000)	3624	7668	2196
crystal size, mm	0.15 × 0.10 × 0.08	0.13 × 0.09 × 0.07	0.10 × 0.08 × 0.04
θ limits, °	0.88 to 25.00	1.38 to 25.00	1.90 to 25.00
index ranges	$-17 \le h \le 17$,	$-16 \le h \le 16$,	$-13 \le h \le 13$
	$-17 \le k \le 17$,	$-35 \le k \le 35$,	$-14 \le k \le 14$,
	$-28 \le l \le 28$	$-30 \le l \le 30$	$-25 \le l \le 25$
reflections collected	37299	102302	18358
independent reflections	16926 [R(int) = 0.1012]	18904 [R(int) = 0.0537]	9330 [R(int) = 0.1007]
completeness to θ = 25.00°	99.4%	100.0%	99.5%
data/restraints/parameters	16926/474/1225	18904/0/1306	9330/351/782
Goodness on fit on F^2	0.930	1.074	0.985
R1 ($I > 2\sigma(I)$)	0.0653	0.0692	0.0744
wR2 (all data)	0.2061	0.1940	0.2394
largest diff peak and hole, e Å^{-3}	2.382 and −2.430	2.146 and −0.722	3.663 and −2.353

resulting brown solution was filtered, precipitated with $[NEt_4]Br$, washed with water (3 × 10 mL) and ethanol (3 × 10 mL), then first extracted with THF (3 × 10 mL) to separate the $[H_{5-n}Rh_{13}(CO)_{24}]^{n-}$ (n = 2, 3) mixture, which represents the main product. Further extraction of the residue with acetone (20 mL) allowed one to obtain the $[H_3Rh_{22}(CO)_{35}]^{5-}$ anion. This solution was layered with hexane (20 mL) and after slow diffusion, black crystals of $[NEt_4]_5[H_3Rh_{22}(CO)_{35}]\cdot 2Me_2CO$ were obtained. It was also possible to obtain black crystals of $[NEt_4]_5[H_3Rh_{22}(CO)_{35}]\cdot 2MeCN$ by slow diffusion of diisopropyl ether into a solution of $[H_3Rh_{22}(CO)_{35}]^{5-}$ in acetonitrile. The salt is soluble in acetone, acetonitrile, DMF, and DMSO and insoluble in nonpolar solvents. Elemental analysis calcd (%) for $[NEt_4]_5[H_3Rh_{22}(CO)_{35}]\cdot 2Me_2CO$, C 24.23, H 2.89, N 1.74, Rh 56.39; found, C 24.31, H 3.00, N 1.82, Rh 56.20.

2. Synthesis of $[H_4Rh_{22}(CO)_{35}]^{4-}$ from $[H_3Rh_{22}(CO)_{35}]^{5-}$. A solution of $[H_3Rh_{22}(CO)_{35}][NEt_4]_5$ in acetone (500 mg, 0.128 mmol) was carefully treated with diluted H_3PO_4. The reaction was monitored via IR and stopped when the carbonyl absorptions at 1975s and 1837ms cm^{-1} of the pentaanion were completely replaced by those of the tetraanion (1992s,1848ms cm^{-1}). The $[NEt_4]^+$ were replaced with $[NMe_3CH_2Ph]^+$ cations by addition of an aqueous solution of $[NMe_3CH_2Ph]Br$ to the acetone solution of $[NEt_4]_4[H_4Rh_{22}(CO)_{35}]$. The resulting suspension was filtered, dried in vacuum, washed with water, and extracted with acetone (20 mL). This latter solution was layered with hexane (20 mL) and after slow diffusion, black crystals of $[NMe_3CH_2Ph]_4[H_4Rh_{22}(CO)_{35}]$ were obtained. Elemental analysis calcd (%) for $[NMe_3CH_2Ph]_4[H_4Rh_{22}(CO)_{35}]$, C 23.40, H 1.78, N 1.46, Rh 58.81; found, C 23.51, H 1.85, N 1.51, Rh 58.72.

3. Synthesis of $[H_2Rh_{13}(CO)_{24}\{Cu(MeCN)\}_2]^-$ from $[H_2Rh_{13}(CO)_{24}]^{3-}$. A solution of $[H_2Rh_{13}(CO)_{24}][NEt_4]_3$ (500 mg, 211 mmol) in 30 mL of MeCN was treated with two equivalents of $[Cu(MeCN)_4][BF_4]$ dissolved in the same solvent. After the slow addition of the latter reactant, the mixture was left reacting under stirring overnight. The resulting solution was filtered, dried under vacuum, extracted with 30 mL of acetone, and crystallized by layering 20 mL of n-hexane. Black crystals of $[H_2Rh_{13}(CO)_{24}\{Cu(MeCN)\}_2][NEt_4]$ suitable for X-ray analysis were obtained. The same reaction can be also carried out in THF. The cluster is soluble in THF, acetone, acetonitrile, and DMF. Elemental analysis calcd (%) for $[H_2Rh_{13}(CO)_{24}\{Cu(MeCN)\}_2][NEt_4]$, C 18.41, H 1.12, N 1.79, Cu 5.41, Rh 56.94; found, C 18.27, H 1.16, N 1.86, Cu 5.37, Rh 56.85.

4. X-ray Data Collection and Crystal Structure Determination of $[NMe_3CH_2Ph]_4[H_4Rh_{22}(CO)_{35}]$, $[NEt_4]_5[H_3Rh_{22}(CO)_{35}]\cdot 2Me_2CO$, and $[NEt_4][H_2Rh_{13}(CO)_{24}\{Cu(MeCN)\}_2]$. Crystal data and details of the data collection and refinement are given in Table 4. The diffraction experiments were carried out at 100 K on a Bruker ApexII diffractometer equipped with a CCD detector by using graphite monochromated MoK_α radiation (λ = 0.71073 Å). An empirical absorption correction was applied on all structures by using SADABS.[30] They were solved by direct methods and refined by full-matrix least-squares based on F^2 using SHELXL97.[31] All non-hydrogen atoms were refined anisotropically, while hydrogen atoms were set geometrically and given fixed isotropic thermal parameters.

dx.doi.org/10.1021/ic101872z |Inorg. Chem. 2011, 50, 2790–2798

The independent units of $[NMe_3CH_2Ph]_4[H_4Rh_{22}(CO)_{35}]$ and $[NEt_4]_5[H_3Rh_{22}(CO)_{35}]\cdot 2Me_2CO$ consist for both in one complete cluster anion, the required cations and in the latter case two solvent molecules. No significant disorder was found, and anisotropic displacement parameter restraints were applied only for the CO ligands and the cations in $[NMe_3CH_2Ph]_4[H_4Rh_{22}(CO)_{35}]$ to obtain a better structural model.

The independent unit in the crystal structure of $[NEt_4][H_2Rh_{13}(CO)_{24}\{Cu(MeCN)\}_2]$ contains one entire cluster plus two $[NEt_4]^+$ molecules with 50% occupancy factors. The carbon atoms in the latter cations were disordered therefore split in two positions in the refinement, using distance and anisotropic displacement parameter restraints.

■ ASSOCIATED CONTENT

Supporting Information. A detailed description of the ESI-MS characterization of $[H_{8-n}Rh_{22}(CO)_{35}]^{n-}$ (n = 4, 5) and $[H_2Rh_{13}(CO)_{24}\{Cu(MeCN)\}_2]^-$, the full list of bond distances for the $[H_2Rh_{13}(CO)_{24}\{Cu(MeCN)\}_2]^-$ anion, the full list of bond distances for the $[H_4Rh_{22}(CO)_{35}]^{4-}$ anion, the crystal structure of the $[H_3Rh_{22}(CO)_{35}]^{5-}$ anion, the full list of its bond distances and all the CIF files of the crystal structures are reported. This material is available free of charge via the Internet at http://pubs.acs.org.

■ AUTHOR INFORMATION

Corresponding Author

*E-mail: cristina.femoni@unibo.it. Phone: 0039-051-2093705. Fax: 0039-051-2093690.

■ ACKNOWLEDGMENT

We thank the University of Bologna and MIUR (PRIN 2008) for their financial support.

■ REFERENCES

(1) Albano, V. G.; Ceriotti, A.; Chini, P.; Ciani, G.; Martinengo, S.; Anker, W. M. *J. Chem. Soc., Chem. Comm.* **1975**, 859–860.
(2) Albano, V. G.; Ciani, G.; Martinengo, S.; Sironi, A. *J. Chem. Soc., Dalton Trans.* **1979**, 978–982.
(3) Martinengo, S.; Ciani, G.; Sironi, A.; Chini, P. *J. Am. Chem. Soc.* **1978**, *100*, 7096–7098.
(4) Ciani, G.; Sironi, A.; Martinengo, S. *J. Organomet. Chem.* **1980**, *192*, C42.
(5) Martinengo, S.; Ciani, G.; Sironi, A. *J. Chem. Soc., Chem. Commun.* **1980**, 1140–1141.
(6) Vidal, J. L.; Schoening, R. C. *Inorg. Chem.* **1981**, *20*, 265–269.
(7) Collini, D.; Fabrizi De Biani, F.; Fedi, S.; Femoni, C.; Kaswalder, F.; Iapalucci, M. C.; Longoni, G.; Tiozzo, C.; Zacchini, S.; Zanello, P. *Inorg. Chem.* **2007**, *46*, 7971–7981.
(8) Vidal, J. L.; Kapicak, L. S.; Troup, J. M. *J. Organomet. Chem.* **1981**, *215*, C11.
(9) Ciani, G.; Magni, A.; Sironi, A. *J. Chem. Soc., Chem. Commun.* **1981**, 1280–1282.
(10) Vidal, J. L.; Schoening, R. C.; Troup, J. M. *Inorg. Chem.* **1981**, *20*, 227–238.
(11) Martinengo, S.; Ciani, G.; Sironi, A. *J. Am. Chem. Soc.* **1980**, *102*, 7564–7565.
(12) Allevi, C.; Heaton, B. T.; Seregni, C.; Strona, L.; Goodfellow, R. J.; Chini, P.; Martinengo, S. *J. Chem. Soc., Dalton Trans.* **1986**, 1375–1381.
(13) Bernardi, A.; Femoni, C.; Iapalucci, M. C.; Longoni, G.; Zacchini, S. *Dalton Trans.* **2009**, 4245–4251.
(14) Collini, D.; Femoni, C.; Iapalucci, M. C.; Longoni, G.; Svensson, P. H. *Inorg. Chim. Acta* **2003**, 321–328.
(15) Bau, R.; Drabnis, M. H.; Garlaschelli, L.; Klooster, W. T.; Xie, Z.; Koetzle, T. F.; Martinengo, S. *Science* **1997**, *275*, 1009–1102.
(16) Gautier, R.; Halet, J.-F. *J. Organomet. Chem.* **1998**, *565*, 217–224.
(17) Fumagalli, A.; Martinengo, S.; Ciani, G.; Masciocchi, N.; Sironi, A. *Inorg. Chem.* **1992**, *31*, 336–340.
(18) Jones, R. A.; Wright, T. C. *Organometallics* **1983**, *2*, 1842–1845.
(19) Sheeman, S. M.; Padwa, A.; Snyder, J. P. *Tetrahedron Lett.* **1998**, *39*, 949–952.
(20) Green, M.; Hankey, D. R.; Howard, J. A. K.; Louca, P.; Stone, F. G. A. *J. Chem. Soc., Chem Comm.* **1983**, 757–758.
(21) Nakatsuji, H.; Onishi, Y.; Ushio, J.; Yonezana, T. *Inorg. Chem.* **1983**, *22*, 1623–1630.
(22) Mingos, D. M. P.; May, A. S. In *The Chemistry of Metal Cluster Complexes*; Sriver, D. F., Kaesz, H. D., Adams, R. D., Eds.; VCH Publishers: New York, 1990; pp 11−119.
(23) Adams, R. D.; Babin, J. E.; Tasi, M. *Inorg. Chem.* **1986**, *25*, 4460–4461.
(24) Demartin, F.; Femoni, C.; Iapalucci, M. C.; Longoni, G.; Zanello, P. *J. Cluster Sci.* **2001**, *12*, 61–74.
(25) Calderoni, F.; Demartin, F.; Fabrizi de Biani, F.; Femoni, C.; Iapalucci, M. C.; Longoni, G.; Zanello, P. *Eur. J. Inorg. Chem.* **1999**, 663–671.
(26) Calderoni, F.; Demartin, F.; Fabrizi de Biani, F.; Femoni, C.; Iapalucci, M. C.; Longoni, G.; Zanello, P. *Eur. J. Inorg. Chem.* **1999**, 663–671.
(27) Zanello, P. *Inorganic Electrochemistry. Theory, Practice and Application*; RSC: Cambridge, UK, 2003.
(28) Mealli, C.; Proserpio, D. M. *J. Chem. Educ.* **1990**, *67*, 399–402.
(29) Keller, E. *Schakal 99*; University of Freiburg: Germany, 1999.
(30) Sheldrick, G. M. *SADABS*; University of Göttingen: Germany, 1996.
(31) Sheldrick, G. M. *SHELX97*; University of Göttingen: Germany, 1997.

■ NOTE ADDED AFTER ASAP PUBLICATION

This paper was published on the Web on February 11, 2011, with a spelling error in the author name Dolzhnikov. The corrected version was reposted on February 16, 2011.